UDC 681.2.088

Krylov A. A., Kuznetsov P. S.

MEMS gyroscope zero drift elimination at different temperature dynamics

The paper describes the physical causes of zero drift and its dependence on temperature. To reveal the temperature dependence of the drift at different heating dynamics, experiments were carried out with different switching intervals. The correlations between the drift and temperature are studied for different switching intervals at a number of significant time points from the switching. A method of drift compensation at different heating dynamics is proposed, which determines the interval closest to the current temperature dynamics.

Keywords: IMU calibration, zero drift of MEMS gyroscopes, Lagrange polynomials

MEMS gyroscopes are adjusted and calibrated as components of the gyro inertial unit (GIU), which is designed as a monoblock case (Fig. 1). The unit accommodates three angular velocity sensors (AVS) comprising micromechanical angular velocity sensing elements of the LL type located inside a glass capsule, and a data processing integrated circuit (ASIC, Application Specific Integrated Circuit). GIU also comprises a programmable microcontroller, which allows for real-rime corrections of MEMS gyroscope readings with regard to revealed systematic errors. The microcontroller memory saves processing algorithms and calibration data allowing for multiple corrections and rewriting in the course of article calibration. GIU generates data at a frequency of 1000 Hz. The instrument's angular velocity measurement range is ±500 °/s.

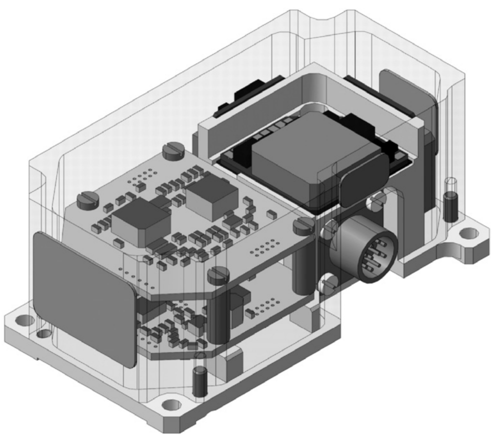

Fig. 1. GIU with its case cover removed

GIU adjustment and calibration involves determination of correction factors for error compensation algorithms by the following parameters:

- non-linearity of scale factor;
- non-orthogonality of GIU axis orientation;
- dependence of bias on linear acceleration;
- initial bias (upon instrument activation) registration;
- temperature zero drift of MEMS gyroscopes.

In the course of gyroscope calibration, the compensation of bias and drift takes most effort as there are many factors affecting the behaviour of such bias and drift, while a large number of available statistic data does not ensure that these errors can be described correctly. Properties of a specific instrument shall be taken into account for more accurate modelling.

In general, bias has two components – initial bias and zero drift. The physical cause of zero drift is a change of dimensions of silicon elements and pressure variation inside the capsule caused by temperature variation. These factors determine variations in the gyroscope self-resonant frequency and, therefore, gyroscope output readings [1, 2]. Temperature variation depends on the effect of external temperature and internal heating of the sensor, which is located close to heat-emitting components.

The above-mentioned factor is frequently observed in compact-size instruments, where accommodation of sensors and heat dissipation from a secondary power supply source is limited. GIU is a compact-size unit, that is why for accurate bias compensation both temperature variation factors shall be taken into account.

It is worth mentioning that the error has both systematic and random components. A systematic component can be eliminated by an algorithm. In this case, the error value will be determined by a random component. A random component cannot be eliminated without interference in internal processes of a MEMS sensor, except for possible application of filtering. This study does not cover the application of filtering.

The gyroscope bias is the difference between gyroscope readings and the zero value provided it is not affected by angular velocity. Zero drift within a certain time period is determined as the difference between maximum and minimum bias values (calculated by the low-frequency component of the signal) within this period.

When studying the behaviour of drift of MEMS gyroscopes included in GIU, we have revealed an evident dependence of the zero signal drift on the temperature measured by the temperature sensor integrated into AVS (Fig. 2 shows the initial bias eliminated mathematically; the temperature is expressed in initial units of the temperature sensor).

Similar results have been obtained in [3–5].

Fig. 2 shows the dependence of bias on internal heating, but the dependence may vary at different structure heating levels that depend on the time passed since the latest activation. The initial bias varies in these conditions as well.

The instrument has stable accuracy characteristics due to resistance to external temperatures and time of the previous activation. For this purpose, it is necessary to simulate the compensation function for a set of temperatures within the operating range (an example of external temperature variation is given in [6]), as well as for various time intervals between instrument activations. The actual scheme allows to measure only temperatures inside MEMS sensors. The time passed since the latest shutdown of the instrument is indirectly estimated based on temperature sensor readings during operation of the instrument. Fig. 2 shows evident similarity of the curves representing temperature rise (caused by internal heating) after the instrument is switched on and the bias is changed.

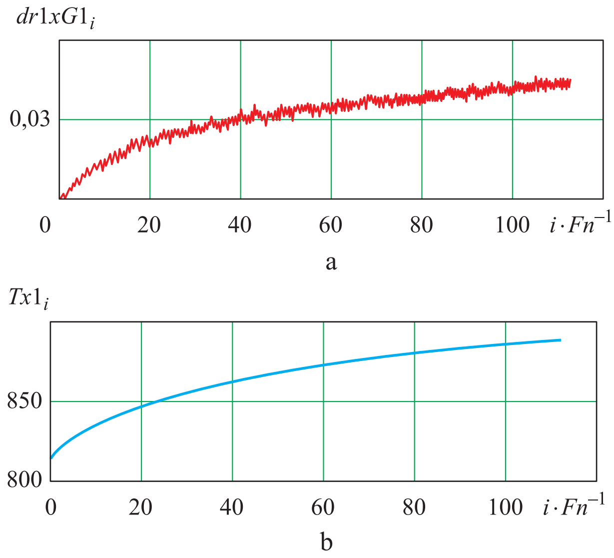

Fig. 2. Dependence of bias on temperature: $dr1xG1$ – low-frequency component of gyroscope signal after activation; $Tx1$ – temperature sensor signal after activation; Fn – instrument data output frequency; i – number of points

In order to study the zero drift, series of 5 activations performed at a certain time interval are analysed (Fig. 3). For our experiment we have selected the following range of intervals between activations: 1, 2, 5, 10, 15, 20, 30 min (axis of abscissas) – a certain interval is used for each series. The drift value is calculated for the entire period of instrument operation (2 min). There is a long-time break (the instrument is switched off in a low-voltage complex device) for 1 h to let the instrument cool down completely. To identify the systematic error, a series is recorded in the same conditions 3 times. Accordingly, values related to each number of activation for a single interval are averaged to be used for further analysis.

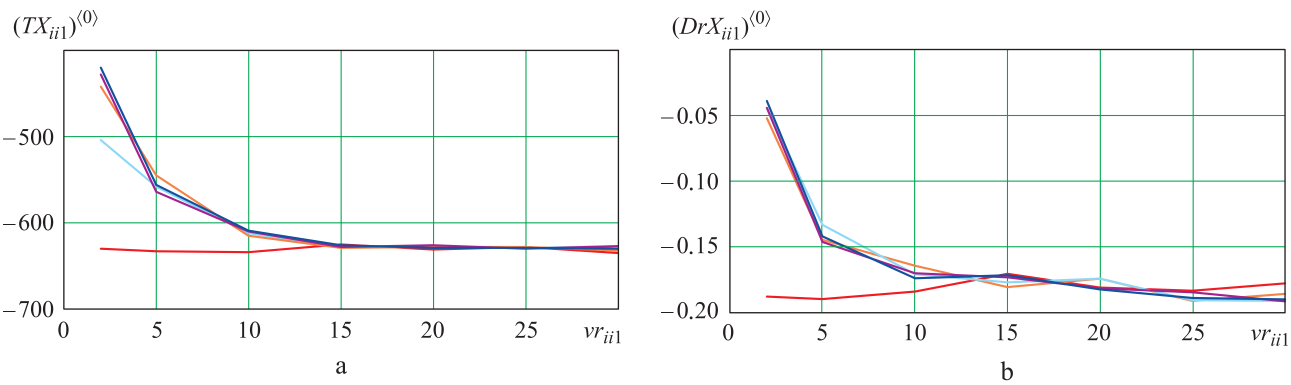

Fig. 3. A graph showing temperature and drift rise registered during series of five activations:
a – temperature sensor readings (1° = 200 units) at different time intervals between activations (axis of abscissas), $ii1$– number of interval between activations; vr_{ii1} – activation interval; $TX_{ii1}{}^{\langle 0 \rangle}{}_k$ – temperature sensor value at the k-th activation; red – $\left[\left(TX_{ii1}\right)^{\langle 0 \rangle}\right]_0$; orange – $\left[\left(TX_{ii1}\right)^{\langle 0 \rangle}\right]_1$; light blue – $\left[\left(TX_{ii1}\right)^{\langle 0 \rangle}\right]_2$; violet – $\left[\left(TX_{ii1}\right)^{\langle 0 \rangle}\right]_3$; blue – $\left[\left(TX_{ii1}\right)^{\langle 0 \rangle}\right]_4$;
b – drift values at different time intervals between activations (axis of abscissas);
$DrX_{ii1}{}^{\langle 0 \rangle}{}_k$ – temperature drift value at the k-th activation;
red – $\left[\left(DrX_{ii1}\right)^{\langle 0 \rangle}\right]_0$; orange – $\left[\left(DrX_{ii1}\right)^{\langle 0 \rangle}\right]_1$; light blue – $\left[\left(DrX_{ii1}\right)^{\langle 0 \rangle}\right]_2$; violet – $\left[\left(DrX_{ii1}\right)^{\langle 0 \rangle}\right]_3$; blue – $\left[\left(DrX_{ii1}\right)^{\langle 0 \rangle}\right]_4$

At intervals between activations over 15 min, the difference either in temperature or in drift between the first activation and the remaining ones becomes indistinguishable, therefore, data registered at instrument activation may be considered independent (see Fig. 3). For the remaining activations, it is reasonable to analyse the effect of partial cooldown on temperature rise and drift variation.

Let us assume that the quotient of zero drift and temperature rise from the beginning of measurements is the correlation dependence at each point (i. e., the temperature in the zero second is assumed to be 0).

Correlation points are determined as follows:

$$gt_i = \frac{g_i}{t_i},$$

where g – low-frequency component of gyroscope values;

t – temperature sensor readings (excluding initial bias);

$i = 0...n$;

n – number of measurements.

According to the requirements to the instrument, the drift measurement time is 2 min.

Fig. 4 shows correlation curves for each number of activation. Note that values are stable for the first activation (as the time interval between series is sufficient to let the instrument cool down). The remaining activations are basically similar, but with some differences that indicate a certain decrease in correlation values for each subsequent activation. As the time interval increases, the difference between activations at adjacent points becomes less distinguishable.

In order to study the dynamics of variation in correlation dependence, we have analysed its values at different time intervals after activation. Fig. 5 shows the curves that illustrate a drift variation for 2, 5, 30, 60, and 120 s (red, violet, blue and orange lines, respectively) for the 5th activation. It is evident that there is a difference between values at different intervals within the series (see Fig. 5).

To take into account all possible scenarios, calibration coefficients for all the intervals may be determined. During operation of the instrument, an ad hoc scenario for application of the coefficients shall be determined. For example, an independent activation (30 min) may be chosen as the initial option with coefficient variation depending on the current temperature rise. To reduce the amount of computations and memory footprint, time intervals over 15 min may be ignored while

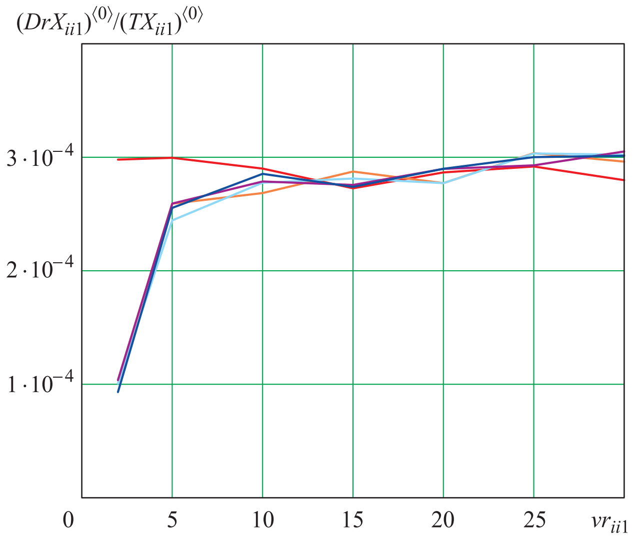

Fig. 4. Correlation dependence values (particular values of drift and temperature sensor readings) at different time intervals between activations (axis of abscissas):
$ii1$ – number of interval between activations; vr_{ii1} – activation interval; ${DrX_{ii1}^{\langle 0\rangle}}_k$ – temperature drift value at the k-th activation; ${TX_{ii1}^{\langle 0\rangle}}_k$ – temperature sensor value at the k-th activation;

red – $\dfrac{\left[(DrX_{ii1})^{\langle 0\rangle}\right]_0}{\left[(TX_{ii1})^{\langle 0\rangle}\right]_0}$; orange – $\dfrac{\left[(DrX_{ii1})^{\langle 0\rangle}\right]_1}{\left[(TX_{ii1})^{\langle 0\rangle}\right]_1}$;

light blue – $\dfrac{\left[(DrX_{ii1})^{\langle 0\rangle}\right]_2}{\left[(TX_{ii1})^{\langle 0\rangle}\right]_2}$; purple – $\dfrac{\left[(DrX_{ii1})^{\langle 0\rangle}\right]_3}{\left[(TX_{ii1})^{\langle 0\rangle}\right]_3}$;

dark blue – $\dfrac{\left[(DrX_{ii1})^{\langle 0\rangle}\right]_4}{\left[(TX_{ii1})^{\langle 0\rangle}\right]_4}$

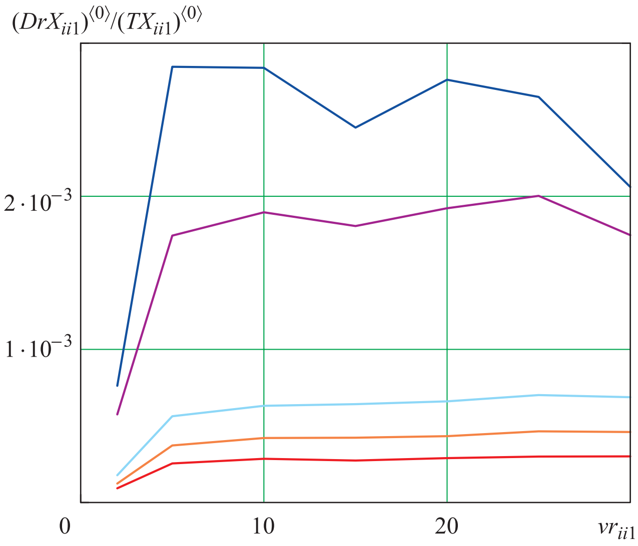

Fig. 5. Graphs showing correlation dependence for int_j = = 2, 5, 30, 60, and 120 s depending on time between activations:
$ii1$ – number of interval between activations; vr_{ii1} – activation interval; ${DrX_{ii1}^{\langle j\rangle}}_k$ – temperature drift value at the k-th activation; ${TX_{ii1}^{\langle j\rangle}}_k$ – temperature sensor value at the k-th activation; $j = 0\ldots4$ – number of interval from activation at which correlation dependence is measured;

red – $\dfrac{\left[(DrX_{ii1})^{\langle 0\rangle}\right]_4}{\left[(TX_{ii1})^{\langle 0\rangle}\right]_4}$; orange – $\dfrac{\left[(DrX_{ii1})^{\langle 1\rangle}\right]_4}{\left[(TX_{ii1})^{\langle 1\rangle}\right]_4}$;

light blue – $\dfrac{\left[(DrX_{ii1})^{\langle 2\rangle}\right]_4}{\left[(TX_{ii1})^{\langle 3\rangle}\right]_4}$; purple – $\dfrac{\left[(DrX_{ii1})^{\langle 3\rangle}\right]_4}{\left[(TX_{ii1})^{\langle 4\rangle}\right]_4}$;

dark blue – $\dfrac{\left[(DrX_{ii1})^{\langle 4\rangle}\right]_4}{\left[(TX_{ii1})^{\langle 5\rangle}\right]_4}$

a 15-min interval is considered independent. With calibration within the entire temperature range, the coefficients are calculated at certain temperature points that cover the entire range.

As the instrument’s operation time is supposed to be two minutes maximum, the temperature variation model can be represented as the initial external temperature plus internal heating.

To compensate the drift during GIU calibration, polynomial approximation is generally used [7]. One of the previous studies offers the piecewise linear approximation [3]. This paper represents a modified approximation, including correlation dependences and dependence on the cooldown time.

A number of points shall be found in accordance with maximum bends of drift curves. Points between such bends are calculated proportionally to the distance to adjacent bends. Before drift approximation, the drift is filtered using the sliding window method at a frequency, which corresponds to the instrument’s operating frequency (1000). The values at reference points are calculated by the following formula

$$d_j = \frac{\sum_{i=0}^{10} gt_{i-5}}{10},$$

where $j = 0\ldots m$;

Table

Drift values obtained during calibration with standard and modified compensation algorithm

Conditions/drift values, °/s		GIU 1			GIU 2		
Type of calibration	Temperature, °C	*X*	*Y*	*Z*	X	*Y*	*Z*
Standard	+30	0.015	0.020	0.012	0.013	0.009	0.006
	+33	0.018	0.017	0.016	0.009	0.014	0.016
	+40	0.008	0.019	0.013	0.010	0.012	0.011
Modified	+30	0.012	0.013	0.010	0.008	0.004	0.005
	+33	0.011	0.01	0.014	0.007	0.008	0.009
	+40	0.006	0.015	0.011	0.005	0.006	0.008

m – number of reference points;

gt_{i-5} – point from correlation array.

Value at any other point at time tx

$$dt_k = d_{j-1} + \frac{d_j - d_{j-1}}{t_j - tx},$$

where $k = 0 \ldots n - m$ – numbers of all points, except reference ones.

The same principle is applied to calculate coefficients for the current temperature. Calibration coefficients are calculated at temperature points beforehand. If a certain point has the current temperature, its coefficients shall be taken; the proportional intermediate value is calculated for the temperature between points:

$$dt_k = d_{T_{j-1}} + \frac{d_{T_j} - d_{T_{j-1}}}{t_{T_j} - tx},$$

where T_j – temperature calibration point higher than current temperature;

T_{j-1} – temperature calibration point lower than current temperature.

To consider the expected number of activation, temperature rise at a certain time point shall be estimated; the final value of dtn_k is also calculated between two adjacent activations using the piecewise linear method:

$$dtn_k = dt_{n1} + \frac{dt_{n2} - dt_{n1}}{dt_{n1} - T},$$

where dt_{n1} – number of activation with higher temperature rise;

dt_{n2} – number of activation with lower temperature rise (it is assumed that the temperature rise will be lower at each subsequent activation);

T – temperature rise at the time interval.

For timely correction, a few time points may be selected, for example, points 2, 5, 30, and 60 s have been selected for the experiment shown in Fig. 4.

The table contains the results of algorithm application in comparison with the standard piecewise linear approximation at temperature points to be calibrated and between them. Temperatures of +30 and +40 °C have been selected for estimation. For these temperatures we have calculated calibration coefficients (reference values) and intermediate temperature of +33 °C.

We may conclude (see Table) that the application of a modified algorithm, including determination and time count between activations improves the drift value by 1.3–2 times in comparison with calibration by means of the standard algorithm (Lagrange polynomials without temperature dynamics).

Bibliography

1. *Lysenko I. Ye.* Vliyanie temperaturnykh i tekhnologicheskikh pogreshnostei na dinamiku trekhosevogo mikromekhanicheskogo giroskopa // Giroskopiya i navigatsiya. 2006. No. 2. S. 6. (Russian)

2. *Vtorushin S. Ye., Arshinova A. A., Nesterenko T. G.* Temperaturniy dreif sobstvennykh chastot mikromekhanicheskogo giroskopa // Vestnik nauki Sibiri. 2014. No. 1, S. 3–5. (Russian)

3. *Krylov A. A., Korniyuk D. V.* Technological approaches to eliminating zero drift of micromechanical gyroscopes // Izvestiya TulGU. Tekhnicheskiye nauki. 2018. No. 5. Pp. 93–98. (Russian)

4. *Prikhodko I. P., Trusov A. A., Shkel A. M.* Compensation of Drifts in High-Q MEMS Gyroscopes

Using Temperature Self-Sensing, Sensors & Actuators // A. Physical. 2013. Vol. 201. Pp. 517–524.
5. *Gulmammadov F.* Analysis, modeling and compensation of bias drift in MEMS inertial sensors // 4th International Conference on Recent Advances in Space Technologies. 2009. Pp. 591–596.
6. *Evstafyev S. D., Rakityansky O. I., Severov L. A., Semenov A. A.* Calibration of information characteristics MMG LL-type // Izvestiya TulGU. Tekhnicheskiye nauki. 2012. No. 7. Pp. 167–172. (Russian)
7. *Lomakin M. A.* Features of error model construction of MEMS sensors for navigation task solution // Engineering Journal of Don. 2014. V. 29. No. 2. Pp. 2–7. (Russian)

Submitted on 29.11.2018

Krylov Aleksey Anatolievich – Software engineer of the 1st category, Joint-Stock Company State Research Institute for Instrument Engineering, post-graduate student, Department 305 Automated complexes of orientation and navigation systems, Moscow Aviation Institute, Moscow.
Science research interests: testing and calibration of navigation devices, MEMS-gyroscopes and accelerometers, development of automated systems.

Kuznetsov Pavel Sergeevich – Candidate of Engineering Sciences, Deputy Head of Department 130, Joint-Stock Company State Research Institute for Instrument Engineering, Moscow.
Science research interests: testing and calibration of navigation devices, MEMS gyroscopes and accelerometers, mechanical and thermodynamic properties of MEMS sensors.

Устранение смещения нуля МЭМС-гироскопов при различной температурной динамике

Описаны физические причины дрейфа нуля и его зависимость от температуры. Для выявления картины зависимости дрейфа от температуры при разной динамике нагрева поставлены эксперименты с разными интервалами включения. Исследованы корреляции между дрейфом и температурой для разных интервалов включения в ряде значимых временных точек от включения. Предложен способ компенсации дрейфа при различной динамике нагрева, определяющий наиболее близкий к текущей температурной динамике интервал.

Ключевые слова: калибровка гироинерциального блока, дрейф нуля МЭМС-гироскопов, полиномы Лагранжа.

Крылов Алексей Анатольевич – инженер-программист 1-й категории Акционерного общества «Государственный научно-исследовательский институт приборостроения», аспирант кафедры 305 «Автоматизированные комплексы систем ориентации и навигации» Федерального государственного бюджетного образовательного учреждения высшего образования «Московский авиационный институт (национальный исследовательский университет)», г. Москва.
Область научных интересов: испытания и калибровка навигационных приборов, МЭМС-гироскопы и акселерометры, разработка автоматизированных систем.

Кузнецов Павел Сергеевич – кандидат технических наук, заместитель начальника отдела 130 Акционерного общества «Государственный научно-исследовательский институт приборостроения», г. Москва.
Область научных интересов: испытания и калибровка навигационных приборов, МЭМС-гироскопы и акселерометры, механические и термодинамические свойства МЭМС-датчиков.